INTERNATIONAL SOCIETY FOR
SOIL MECHANICS AND
GEOTECHNICAL ENGINEERING

This paper was downloaded from the Online Library of the International Society for Soil Mechanics and Geotechnical Engineering (ISSMGE). The library is available here:

https://www.issmge.org/publications/online-library

This is an open-access database that archives thousands of papers published under the Auspices of the ISSMGE and maintained by the Innovation and Development Committee of ISSMGE.

The paper was published in the proceedings of the 10th European Conference on Numerical Methods in Geotechnical Engineering and was edited by Lidija Zdravkovic, Stavroula Kontoe, Aikaterini Tsiampousi and David Taborda. The conference was held from June 26th to June 28th 2023 at the Imperial College London, United Kingdom.

To see the complete list of papers in the proceedings visit the link below:

https://issmge.org/files/NUMGE2023-Preface.pdf

Proceedings 10th NUMGE 2023
10th European Conference on Numerical Methods in Geotechnical Engineering
Zdravkovic L, Kontoe S, Taborda DMG, Tsiampousi A (eds)

© Authors: All rights reserved, 2023
https://doi.org/10.53243/NUMGE2023-361

Regional subsidence effects in tunnel-soil-structure seismic interaction

J. M. Mayoral[1], M. Pérez[1], M. Alcaraz[1],

[1]*Department of Geotechnics, Institute of Engineering, Universidad Nacional Autonoma de Mexico, Mexico City, Mexico*

ABSTRACT: Recent numerical studies have shown the importance of the interaction between underground and surface structures. Although the results have been revealing, it has not been considered that this interaction can change over time in areas susceptible to regional subsidence. In this paper, the performance of systems comprised by on-ground and underground structures subjected to seismic loads and regional subsidence is evaluated in the soft clays of Mexico City. The analyses are made by three-dimensional finite difference models, coupling the hardening-soil model to simulate consolidation due to the presence of structures and regional subsidence, with a hysteretic model to consider the degradation of stiffness and increase in damping during the seismic load. To simulate subsidence, the sinking and piezometric depletion rates of the studied area are considered. The analyses conducted involve the evaluation of the seismic performance of the system of structures at different times during its economic life, considering the simulation of the consolidation process.

Keywords: Subsidence, soil-structure interaction, tunnel, soft clay, numerical models.

1 INTRODUCTION

Recently, transport strategic infrastructure has increased rapidly in Mexico City. Due to the connectivity required by several transport systems, the interaction between surface and underground structures has become increasingly common, in the so-called Transit Transfer Stations, TTS. This condition leads to interdependent multiple hazards that can impact the infrastructure systems, which, in turn, are also affected by changes in the initial geotechnical conditions associated to regional subsidence during the economic life of the infrastructure. Additionally, it is crucial to properly assess the seismic demand expected to occur in the strategic infrastructure (i.e., bridges, overpasses, buildings, tunnels, transfer transit stations, among others), especially in densely populated areas located in seismically active regions such as Mexico City. It has been observed that underground structures change the propagation pattern of the arriving seismic waves from the source to the site, affecting the free-field and near field seismic response (Mayoral & Mosqueda, 2020, Wang et al., 2017, Amorosi & Boldini, 2009) and the dynamic pressures in tunnel walls during seismic loading (Liu et al., 2022).

On the other hand, assessing the seismic performance of structures subjected to regional subsidence induced by excessive groundwater extraction is critical. This is because excessive settlements and distortions are the main source of poor long-term behaviour, as it causes the collapse and cracking of the structures (Ovando-Shelley et al., 2003; Rodríguez et al., 2015). However, the complexity of the problem is challenging, and there is no closed-form solutions to analyse it. So, advanced numerical methods are required to investigate the tunnel-soil-structure interaction, with a constitutive model capable of simulating the gradual soil hardening and the nonlinearities developed during the cyclic loads.

This paper presents three-dimensional analyses of a section of a Transfer Transit Station consisting of a cut-and-cover tunnel and a two-level interchange building which crosses perpendicularly the TTS. The analyses conducted involve the evaluation of the seismic performance of the system of structures at different times during it economic life, considering the simulation of the consolidation process. Those were made through 3D finite difference models, coupling the plastic-hardening model (Schanz et al., 1999) (hardening-soil, HS) with the hysteretic Sig3 model, both available in the FLAC^{3D} software (Itasca, 2009).

2 CASE STUDY

The case study is located in the north-eastern part of Mexico City. The soil profile at the studied site presents a desiccated shallow crust of clay with filling material (Crust) extending up to a depth of 4.2 m, which is underlain by a very soft clay layer (Clay1) about 16.1 m thick. Underlying the clay, there is a 1.9 m thick layer of very dense sandy silt (SS1), which rests on top of a soft clay layer (Clay2) that goes up to 30.6 m in depth. Underneath this elevation, a competent layer of about 3.4 m of very dense silty sand (SS2) is found resting on a 6 m layer of soft clay (Clay3). Finally, a highly competent layer of dense silty sand is found (SS3) up to 70 m depth. Table 1 presents the geotechnical parameters defined from triaxial compression and oedometer laboratory tests. The shear wave velocity profile (see Fig. 2(d)) was estimated using the expressions in terms of the tip penetration resistance, qc, measured with the Cone Penetration Test (Shahri & Naderi, 2016). The topographic surveying at the site shows that the sinking rate is about 3 cm/year.

Table 1. Geotechnical parameters used in the numerical model.

Layer	Depth (m)	γ[kN/m^3]	e_0	PI [%]	*k* [m/s]	Model	Su [kPa]	φ' (°)	E_{50} (kPa)	E_{oed} (kPa)	E_{ur} (kPa)	OCR
Crust	4.2	11.67	5.53	50	7.7e-10	MC	20	35	2400	-	-	-
Clay1	7.0	11.38	5.50	200	1.1e-9	HS	5	38	1000	422	7161	1.30
	9.0	11.58	5.75	170	1.4e-9	HS	5	38	1400	379	7259	1.19
	11.5	11.38	5.60	150	1.1e-9	HS	5	38	1680	481	6867	1.25
	14.0	12.95	2.86	120	4.4e-10	HS	5	38	2680	701	10595	1.32
	17.0	13.44	2.62	110	4.7e-10	HS	5	38	3680	1144	11036	1.25
	20.3	12.85	2.86	100	8.1e-10	HS	5	40	2350	760	8535	1.03
SS1	22.2	14.72	0.96	15	8.0e-6	MC	95	30	13000	-	-	-
Clay2	24.0	13.03	4.04	80	1.4e-10	HS	5	40	2700	650	8093	1.27
	26.8	13.58	3.02	80	2.2e-10	HS	5	42	2990	1148	13734	1.12
	30.6	13.73	2.50	60	1.0e-10	HS	5	42	7000	2050	20600	1.04
SS2	32.0	17.03	0.86	15	8.0e-9	MC	115	35	15660	-	-	-
	34.0	17.00	0.86	15	8.0e-9	MC	115	35	22000	-	-	-
Clay3	40.0	14.00	1.89	70	1.0e-10	HS	5	42	9000	2250	27470	1.05
SS3	70.0	18.00	0.70	20	8.0e-9	MC	190	35	98100	-	-	-

where γ is the volumetric weight, e_0 is the void ratio, PI is the plasticity index, k is the coefficient of permeability, Su is the shear undrained resistance, φ' is the effective friction angle, OCR is the over consolidation ratio, and E_{50}, E_{oed}, E_{ur} are the stiffness parameters of the HS model.

The cut-and-cover tunnel is made of 0.4 m thick concrete walls, with a compression strength, f'c, of 30 MPa, with a cover of 1.70 m depth. Above, a two-level interchange building is placed crossing perpendicularly the main body of the TTS. Common structural steel typologies comprised the structural elements of the building (i.e. columns and beams). The foundation is divided into two sections (i.e., south and north sections, see Fig. 1), and consists of a box foundation with concrete slabs and walls with f'c=30 MPa, complemented with friction piles commonly used to reduce differential settlements and structure emersion associated with regional ground subsidence. Figure 1 shows a schematic representation of the case study.

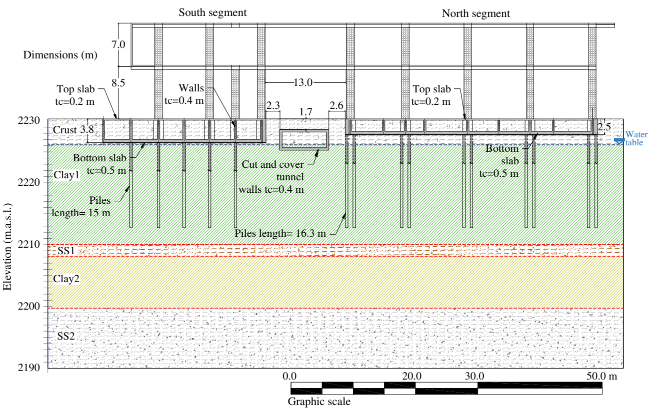

Figure 1. Schematic representation of the structures and the soil profile.

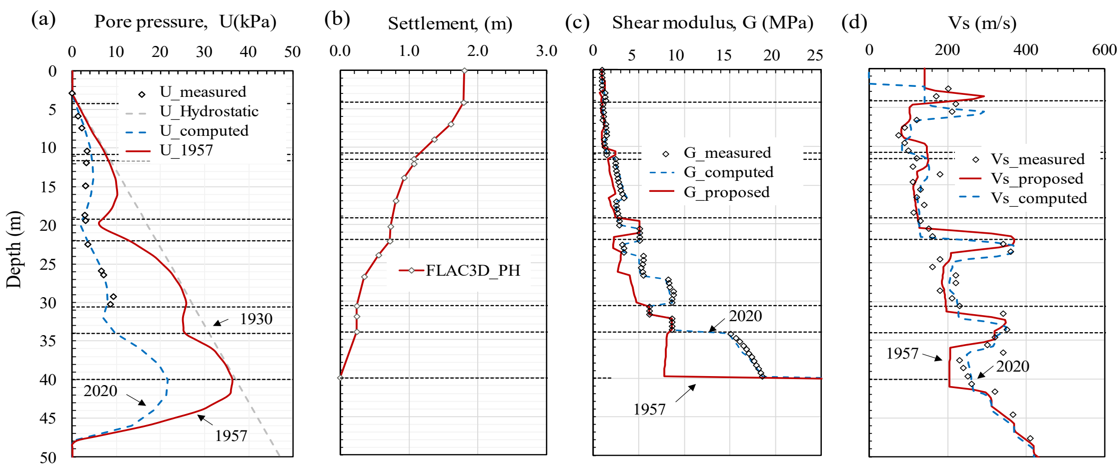

Figure 2. (a) Pore pressure profiles measured and computed for different ages in the study area, (b) settlement profile computed by means of the numerical model from 1957 to 2020, (c) measured and computed static shear modulus for different ages, and (d) shear wave velocity profiles measured and computed for different ages.

3 NUMERICAL SIMULATION

The tunnel-soil building seismic interaction was studied by a series of three-dimensional finite difference numerical models developed with FLAC^{3D} (See Fig.3). The columns and beams of the structure were simulated with BEAM elements, decks, slabs, and walls with SHELL elements, and the friction piles with PILE elements.

The high plasticity clay was modelled with the HS model, and the silty sands were with Mohr-Coulomb, MC. The parameters required by the constitutive model were defined through calibration using laboratory and field tests data available from the site. These are shown in Table 1. The model consists of 358218 three-dimensional elements representing the soil mass where the underground and the surface structure were projected. In addition, several control points were located in sections of interest in the model (around foundations, around the tunnel, cover roof, and free field) to monitor displacements, accelerations, and stresses during the simulations.

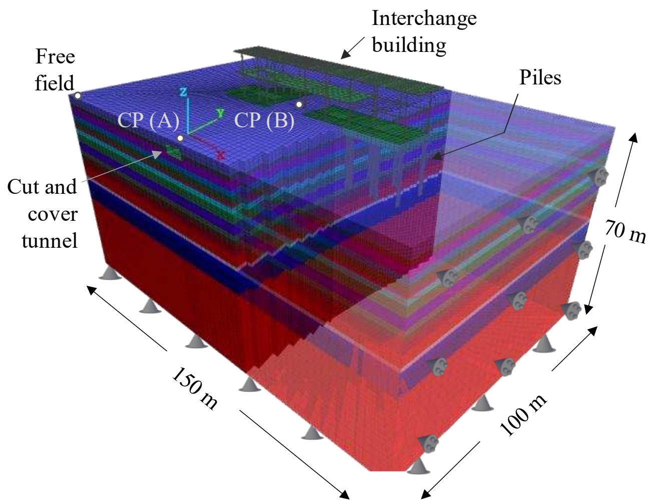

Figure 3. Three-dimensional finite difference model considering the interchange building and the cut and cover tunnel, and control points location.

3.1 *Subsidence and piezometric withdrawn associated with water extraction rates*

Following the methodology proposed by Mayoral et al., (2017), an iterative approach based on back-analyses was implemented to properly represent the sinking and the piezometric depletion rates of the site with the numerical model. The calibration consisted of replicating the known pore pressure isochrones at several ages, starting from the hydrostatic condition, estimated for the year 1930. On the other hand, the settlement caused by those pore pressure changes was computed with the numerical model, where the compressibility parameters were calibrated until reproduce the sinking rate measured for each time interval.

The measured values of pore pressure are shown in Figure 2(a), as well as the estimated piezometric condition for the year 1957 based on former research (Marsal & Mazari, 1959). Figure 4(b) presents the computed settlement from 1957 to 2020 (i.e., 1.85 m), considering a sinking rate of 3 cm per year. Figures 4(c) and 4(d) also present the measured and computed static shear modulus and shear wave velocity profiles measured and computed for different ages. Likewise, the shear wave velocity profile at the end of the consolidation process was estimated with the relationship established by Benz & Vermeer (2007).

3.2 *Dynamic analysis*

The strong ground motion recorded during September 19, 2017, Puebla-Mexico earthquake at station CU01 (located on basalt rock) was used as input in the dynamic analyses. Figure 4 shows the measured accelerations for the orthogonal components; both were considered in the seismic response analyses.

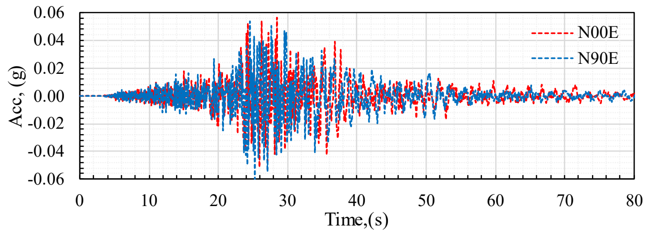

Figure 4. Accelerations time histories recorded by the station CU01 during the September 19, 2017, Puebla-Mexico earthquake.

To establish the input motion applied at the base of the model, the surface ground motion was deconvolved with the program SHAKE (Schnabel et al., 1972). To avoid wave reflections during the dynamic simulation, quiet boundary conditions were defined at the base of the model using the formulation from Lysmer & Kuhlemeyer (1969). Free field boundaries were considered using the formulation available in FLAC^{3D}.

To consider the stiffness degradation and the increase in damping of the soil during the ground shaking, the hysteretic model denominated Sig3, available in FLAC^{3D}, was used. The curves defined for each layer are shown in Figure 5, along with the corresponding expected theoretical curves, defined according to the confinement stress, σc, plastic index, PI, and type of soil compiled in Table 2. The mechanical behaviour of the soil was characterized with the aforementioned curves and the Mohr-Coulomb failure criterion, considering the undrained parameters of the soil. The dynamic analyses were made before and after the consolidation.

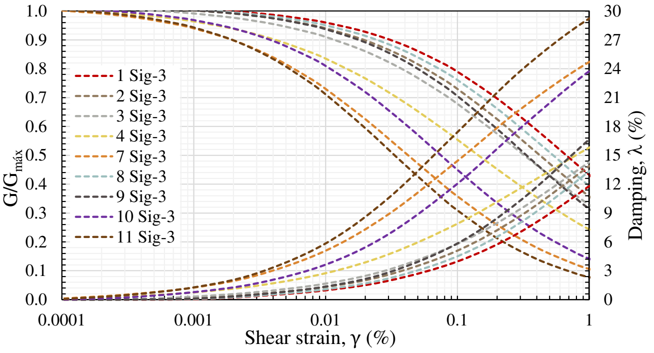

Figure 5. Normalized shear modulus degradation, G/G_{max}, and damping, λ, curves.

Table 2. Normalized shear modulus degradation and damping curves used for each layer.

#	Theoretical backbone	Layer
1	Gonzáles & Romo(2011) PI=200 σ'c=84kPa	Clay1
2	Gonzáles & Romo(2011) PI=170 σ'c=132kPa	Clay1
3	Gonzáles & Romo(2011) PI=150 σ'c=173 kPa	Clay1
4-6	Gonzáles & Romo(2011) PI=110 σ'c=280 kPa	Clay1
7	Darendeli & Stokoe(2001) PI=50 σ'c=34 kPa	Crust
8	Vucetic & dobry(1991) PI=80	Clay2
9	Vucetic & dobry(1991) PI=60	Clay2
10	Darendeli & Stokoe(2001) PI=15 σ'c=362 kPa	SS1, SS2
11	SAND, Lower (Seed & Idriss 1970)	SS3

4 RESULTS AND DISCUSSION

4.1 *Static long-term behaviour*

The consolidation analysis with the presence of structure was carried out considering the total depletion of the pore pressure starting from the year 2020. According to the computed settlement of 0.45 m and the sinking rate, this condition could be reached in 15 years. Figure 6(a) shows the deformed mesh of the model at the end of the simulation. As can be seen, all the structures presented an apparent emersion of different magnitudes, reaching differential settlements until 0.2 m with the adjacent zones. Figure 6(b) depicts several problems that could be generated in the long term by subsidence and differential settlement, such as the generation of down-drag forces in piles, the formation of gaps under the slab, and surface cracking between the emerging structures and the adjacent areas. Therefore, to achieve a better long-term performance of the system, it is strongly recommended to design the structures to follow the sinking rate associated with regional subsidence as close as possible, in order to avoid differential settlements.

4.2 *Seismic response and interaction effects*

Initially free filed conditions site response was established. For comparison purposes, the seismic response of the assumed 1957 initial condition was also calculated. Figure 7 shows the response spectra obtained at the surface from the different ages considered, as well as the response spectrum of the input motion. From these results, two main effects can be highlighted, the shortening of the fundamental period of the soil, Ts, and the amplification of the spectral ordinates. The first one is due to geometrical changes of the soil strata and hardening of the soil matrix, and the second one is because the energy of the input motion concentrates in low periods, so as the Ts get closer to these, the seismic response is amplified (Mayoral & Mosqueda, 2020, 2021).

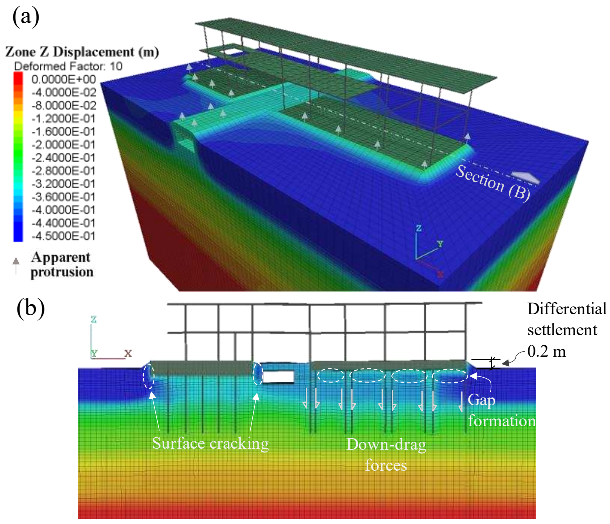

Figure 6. (a) Settlement at the end of the simulation, (b) Cutting plane on section (B) showing the different potential problems generated by the regional subsidence.

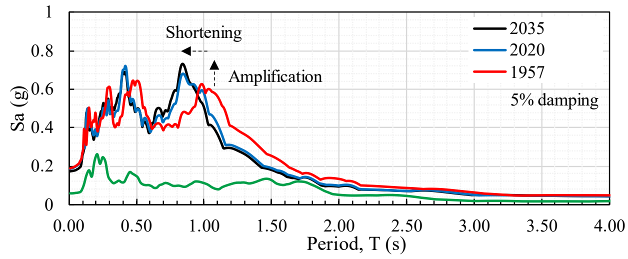

Figure 7. Response spectra obtained by the dynamic simulation at different ages.

Following the analysis process, the ground shaking simulation was carried out considering the presence of the structures in the year 2020 and 2035. According to Mayoral & Mosqueda (2020), the surface ground motion variability in the tunnel's longitudinal direction is not as significant as in the transversal direction, so special attention was paid to this direction. Figure 8 shows the comparison between the Fourier spectra obtained in the structure before and after the consolidation. It can be observed that the fundamental period of vibration of the structure is around 0.33 seg (3Hz), where the main amplification occurs. Also, this amplification increases in the 2035 condition due to the fundamental frequency of the soil getting closer to that of the structure.

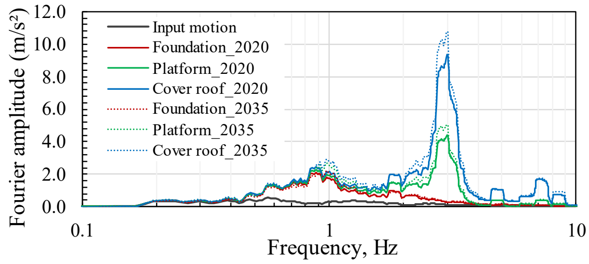

Figure 8. Fourier spectra obtained by the dynamic simulation in the different levels of the structure at different ages.

Transfer functions, TF, between control points (A) and (B) and the Free field were estimated to assess the impact of the structure on the seismic response. Figure 9(a) shows the TFs obtained for the year 2020, where it can be noticed that the main variations (i.e., 20% of amplification or attenuation) of the seismic response occur after 2 Hz, thus only lower structures above the tunnel with short structural periods are expected to be affected. Another noticeable effect is the additional attenuation associated with the presence of the building around 3 Hz, which is the characteristic frequency of vibration of the structure in the transversal direction. This effect suggests that the motion in this zone is restricted by the box foundations of both building segments, so a beneficial interaction occurs. Regarding the response computed for year 2035, shown in Figure 9(b), this effect decreases, which can be associated with the apparent emersion of the building that causes the partial unconfinement of its box foundation.

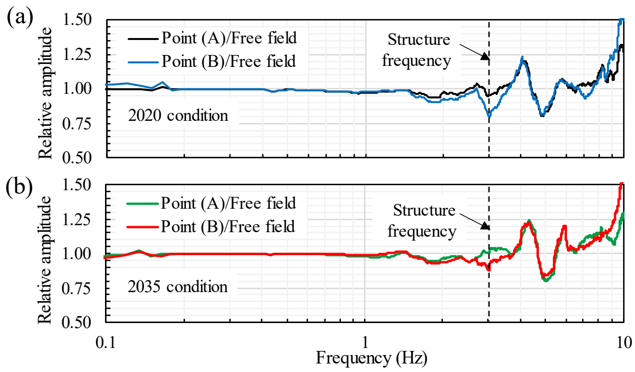

Figure 9. Transfer functions between control points and Free field (a)before and (b) after the consolidation.

Due to the ground deformation restriction due to the adjacent building foundations, an increase in the lateral earth pressures acting on the tunnel is expected. The envelopes of lateral forces acting on the tunnel walls during the ground shaking were obtained. Figure 10(a) shows the results obtained in the 2020 condition, where can be observed the comparison between the pressures reached in the section of control points (A) and (B). As can be seen, the zones of the walls that corresponds to the depth of the box-foundations are the zones where the pressure increased. This effect is more noticeable on the left side due to deep of the box foundation of the short segment of the building.

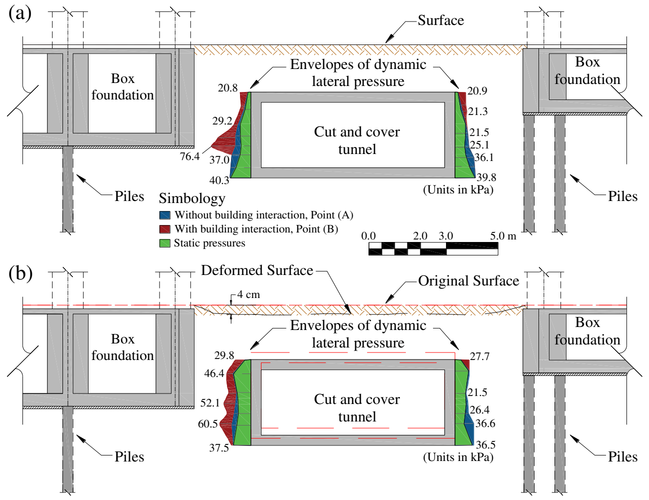

Figure 10. Static and dynamic lateral pressures developed in the tunnel walls (a) year 2020 and (b) year 2035.

For the 2035 condition, shown in Figure 10(b), the pressures also increase with the presence of the box foundations. Nevertheless, the pressures are distributed uniformly along the wall and in the section of point (A). This can be associated with the hardening of the soil and the increase of the effective stresses caused by the consolidation process. Also, it can be seen that the boxes and the tunnel have less interaction because of the relative displacements between them.

Another interesting aspect to verify is the sitffness degradation and the damping variation in the system during the ground shaking. The hysteretic model sig3, available in FLAC^{3D}, was used. Due to the level of strains expected, control points were located around the structures in which G/Gmax values were stored during the simulation. Figure 11(a) shows the zones where the values were stored, and Figure 11(b) presents the corresponding values by each zone.

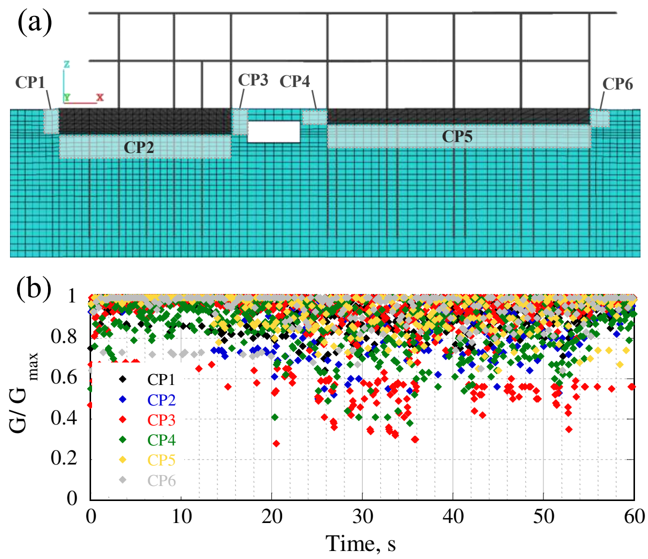

Figure 11. (a) Location of zones where the stiffness degradation was monitored and (b)G/G_{max} values stored during simulation.

Upon analyzing the recorded values of stiffness degradation in zones CP3 and CP4, it can be noted that the attenuation between the box foundations is because of the high damping developed. The stiffness degradation reaches values up to 0.3 in these zones, thus the corresponding damping are very high, in the order of 15 to 20%, depending on the damping curve. Regarding the other zones, the values are concentrated in the range of 0.6 to 1. However, the variation of G/Gmax values during ground shaking is significant, which can not be simulated with the equivalent linear method. So, adopting a fully nonlinear approach is essential to evaluate this type of system where considerable interaction effects are developed.

5 CONCLUSIONS

Several problems induced by regional subsidence and interaction effects developed during seismic loading were discussed. Regarding the static long-term performance, it was observed that the building could emerge up to 0.2 m with respect to the adjacent soil. To mitigate the discussed problems, it is necessary that both structures follow the sinking rate, which can be achieved by adjusting the weight of the structure or the number of friction piles.

In the case of dynamic behaviour, the seismic demand of the building increase when consolidation occurs after 15 years due to the migration of the fundamental frequency of the soil, that gets closer to that of the structure. About the interaction effects, it is observed that the motion of the tunnels is restricted by the box foundations, which generates an increase in the dynamic lateral pressures acting on the tunnel walls, which can be up to 100%. Also, the distribution of such pressures changes when consolidation occurs, so these fluctuations must be considered in the reinforcements of the tunnel's walls. Another significant aspect observed in the simulation was the additional stiffness degradation and damping that occurs in the zones between the box foundations and the tunnel, which directly affects the seismic response of the building. With these aspects, adopting a completely nonlinear approach is important to evaluate this type of system where considerable interaction effects are developed.

6 REFERENCES

Amorosi A, Boldini D. 2009. Numerical modeling of the transverse dynamic behaviour of circular tunnels in clayey soils. Soil Dynam Earthq Eng;59:1059–72. 2009.

Benz, T., & Vermeer, P. A. (2007). Zuschrift zum Beitrag" Uber die Korrelation der odometrischen und der" dynamischen" Steifigkeit nichtbindiger Boden" von T. Wichtmann und Th. Triantafyllidis (Bautechnik 83, No. 7, 2006). *Bautechnik*, *84*(5), 361–364.

Darendeli MB, Stokoe KH., II. (2001) Development of a new family of normalized modulus reduction and material damping curves, Geotechnical Engineering Report GD01-1, University of Texas at Austin, Austin

Gonzalez, C., & Romo, M. P., 2011. Estimacion de propiedades dinamicas de arcillas, Revista de Ingenieria Sismica 84 (2011), 1-23.

Itasca, 2009. FLAC^{3D}. Minneapolis, Minnesota, USA: Fast Lagrangian Analysis of Continua in 3 Dimensions, User´s Guide.

Liu, B., Zhang, D., Li, X., & Li, J. (2022). Seismic response of underground structure–soil–aboveground structure coupling system: Current status and future prospects. *Tunnelling and Underground Space Technology*, *122*(January), 104372.

Lysmer, J., Kuhlemeyer, R. L. (1969). Finite dynamic model for infinite media. Journal of the Engineering Mechanics Division, 95(4), 859–878.

Marsal, R.J. & Mazari, M. (1959). The Subsoil of Mexico City. Contribution to First Panamerican Conf. on Soil Mechanics and Found. Eng., Mexico City

Mayoral J.M. & Mosqueda G. 2021. Foundation enhancement for reducing tunnel-building seismic interaction on soft clay. Tunn and Und Space Tech 115, 104016

Mayoral, J. M., & Mosqueda, G. (2020). Seismic interaction of tunnel-building systems on soft clay. *Soil Dynamics and Earthquake Engineering*, *139*(September), 106419.

Mayoral JM, Castañón E, Albarran J. (2017). Regional subsidence effects on seismic soil-structure interaction in soft clay". Soil Dyn and Earth Eng 103:123–140

Ovando-Shelley, E., Romo, M. P., Contreras, N., & Giralt, A. (2003). Effects on soil properties of future settlements in downtown Mexico City due to ground water extraction. *Geofisica Internacional*, *42*(2), 185–204.

Rodríguez Rebolledo, J. F., Auvinet-Guichard, G. Y., & Martínez-Carvajal, H. E. (2015). Settlement analysis of friction piles in consolidating soft soils. *DYNA*, *82*(192), 211–220.

Shahri, A., Naderi, S. 2016. Modified correlations to predict the shear wave velocity using piezocone penetration test data and geotechnical parameters: a case study in the southwest of Sweden. Innov. Infrastruct. Solut. 1, 13

Schanz, T., Vermeer, P. A., & Bonnier, P. G. (1999). The hardening soil model: Formulation and verification. *Beyond 2000 in Computational Geotechnics. Ten Years of PLAXIS International. Proceedings of the International Symposium, Amsterdam, March 1999.*, 281–296.

Schnabel P.B., Lysmer J. & Seed H.B. 1972. SHAKE: a computer program for earthquake response analysis of horizontally layered sites, software.

Seed H.B. & Idriss I.M. 1970. Soil Moduli and Damping Factors for Dynamic Response Analyses, Tech. Rep.197109, California Univ., Berkeley. Earthquake Engineering Research Center.

Vucetic, M. and Dobry, R. [1991] "Effect of soil plasticity on cyclic response", Journal o Geotech. Engineering, ASCE, 1991, vol. 114, No. 1

Wang G, Yuan M, Ma X, Wu J. 2017. Numerical study on the seismic response of the underground subway station-surrounding soil mass-ground adjacent building system. Front Struct Civ Eng;11:424–35